Robust Nonlinear Economic MPC Based Management of a Multi Energy Microgrid

Josip Vasilj, Damir Jakus, and Petar Sarajcev

***Abstract*—In this paper, the nonlinear economic model predictive control based energy management of a multi-energy microgrid is presented. The microgrid is composed of the district heating system with a cogeneration power plant supplying both the heat and the electricity demand of residential buildings with photovoltaic sources. Furthermore, access to liberalized heat and electricity market is assumed. This kind of environment requires consideration of the economical aspects, the technical aspects, the safety/quality of supply, and consumer preferences. The major contributions introduced in the presented approach are the following. A nonlinear formulation is adopted to capture the nonlinear thermal models and the nonlinear algebraic model of the heat supply network. The second major contribution is the economic character of the objective following the assumption of a liberalized market environment. Such formulation accounts for the specifics of the energy market organization. Finally, the stochastic nature of the planning problem is introduced through a practical robust formulation. The results obtained on a representative case study clearly show the benefits of the proposed approach compared to the traditional energy management approach.**

***Index Terms*—Multi-energy systems, microgrid, model predictive control, robust control, District heating.**

I. Introduction

MODERN energy supply systems require highly efficient energy conversion systems in order to reduce the human impact on the environment. Among such systems, cogeneration power plants are still the foundation of district heating systems. Their ability to utilize the energy extracted from the fuel in several phases for both the electrical and heat energy production results in a highly efficient energy conversion process with eta reaching up to 80% [1]. Another important change in trend is the development of smaller-scale CHP plants appropriate for smaller communities or industrial facility [2]. This development puts CHP plants into a new context, the context of multi-energy microgrids. By definition, the microgrid is the set of interconnected loads and distributed energy sources that act as a single controllable entity with respect to the grid [3]. This definition can be further expanded to include heat energy and form the multi-energy microgrid. As this definition suggests, the interaction with the grid is the basic determinant of the microgrid concept. This interaction can be seen through the exchange of energy in an organized energy market. The basic contribution we propose here is the improvement in the management of the described multi-energy microgrid.

Although cogeneration power plants connect heat and electric energy supply systems, often, they are considered separately, especially in the context of energy management. Typically, a priority is given to one form of energy and the other is determined based on the maximal energy that can be extracted at this operation point. With the recent advancements in system monitoring, communicating, controlling, and forecasting it is possible to develop more advanced energy management schemes that can utilize available information for more economically and technically efficient energy supply. The ideal control scheme that can account for all of the characteristics of district heating systems and cogeneration power plants is the model predictive control. Furthermore, the economic model predictive control concepts [4] could contribute to even greater efficiency when applied to the cogeneration energy conversion process control. In this paper, we show that the economic nonlinear MPC delivers the best results regarding the economic efficiency of the energy supply while satisfying all of the safety requirements. The stochastic nature of the weather/market-driven planning requires robustness in control in order to ensure flexibility for extreme scenarios. A practical form of robustness is introduced ensuring that the system will be able to withstand the outer hull of the scenario space without violating operational and safety conditions. It is important to state that no strict feasibility guarantee is ensured for this approach. Rather, robustness here indicates a control dependent on extreme scenarios. The proposed MPC scheme represents a comprehensive control framework that exploits the full potential of cogeneration power plants.

A. Literature Overview

In the broader context, we would like to mention several papers covering the problem of microgrid management. This problem has been approached primarily from the electrical side with a typical case of electric energy source mixture [5] while the heat component is rarely considered. Other omnipresent topics include the microgrid modeling [6], the operation under different regimes [7], or the application of novel algorithms for management [8]. Compared to these topics, the problem of joint electric and heat management is less present.

In relation to our work, we would like to give a brief overview of the following publications. In [9], authors present a mixed-integer linear programming based model for stochastic scheduling of microgrids with CHP plants. However, the heat component is considered only as a passive demand and the

Manuscript received April 21, 2020; revised September 4, 2020 and November 6, 2020; accepted December 7, 2020. Date of publication December 22, 2020; date of current version May 21, 2021. Paper no. TEC-00 402-2020. *(Corresponding author: Josip Vasilj.)*

The authors are with the University of Split, HR-21000 Split, Croatia (e-mail: josip.vasilj@fesb.hr; damir.jakus@fesb.hr; petar.sarajcev@fesb.hr).

Color versions of one or more figures in this article are available at https://doi.org/10.1109/TEC.2020.3046459.

Digital Object Identifier 10.1109/TEC.2020.3046459

system model is not dynamical. In [10] the authors consider a combined CHP and HVAC system and perform Genetic algorithm based optimization. Again, the model is lacking dynamics and detailed modeling of the heat demand. In [11], [12], the emphasis is put on the economic side of the microgrid operation, where [12] puts the problem into the MPC context. Both papers neglect the system dynamics and the heat demand model. The major issue in the control frameworks presented so far is that the heat side of the system is considered through the demand curve. In [13], the dynamics of the heat demand are modeled through detailed modeling of the building heat exchange. However, the proposed model adopts linear MPC and approximates various nonlinearities. Furthermore, the presented model neglects the heat network. Finally, a similar problem was investigated in [14], where authors adopt a data-driven robust predictive control for district energy control. The focus in their approach is put on the disturbance identification based on the historical data. The obtained model is approximated by a finite-dimensional linear program. In relation to the approach presented in [14], we put a greater focus on the detailed nonlinear model of the district heating system with a detailed modeling of market relations and less focus on the disturbance integration.

The problem of district heating network modeling in the context of joint electric/heat supply has been considered in [15]. A detailed nonlinear model of the district heating network and the electric network is presented. The focus [15] is the analysis of the combined electric/heat network and not the control. Furthermore, the demand is modeled as static heat loads. This model will serve as the basis of the hydraulic component of the district heating network model.

B. Contributions

The first major contribution is related to the application of non-linear economic MPC which allows for a more accurate representation of the model and the economic consequences. Numerous nonlinearities encountered in the mathematical model of the district heat supply system can be handled with this scheme. However, the complexity of this scheme is far greater compared to the traditional linear MPC scheme, but with the assumed development of the computational power, we expect for this control scheme to be a real-time solution.

The second major contribution is the economic nature of the objective following the typical liberalized electric and heat energy market organization. The power plant together with its local consumers having their specific energy structure (a form of a microgrid) participate as a single entity in the larger electric/heat energy market. The ability to transfer the economic consequences of the system operation back to the process control sets a realistic objective in the system control.

The third major contribution is the incorporation of the detailed network and building model allowing for the exploitation of the building thermal dynamics and utilization of the weather/habit forecasts.

The last major contribution is the robust formulation of the original problem in order to respond to uncertainties in forecasts. Namely, weather parameters trajectories can deviate from the expected and the microgrid needs to be able to respond to these uncertainties.

II. Overview of the System

The system under consideration is depicted in Fig. 3. It includes the cogeneration power plant as the central energy subject on the production side. The demand side of the system includes buildings connected to the district thermal grid. These buildings are small energy systems of their own, absorbing the solar power and demanding thermal energy based on the habits of its residents. The same holds for the electric energy; buildings have photovoltaic panels integrated on rooftops and the residual electric consumption is highly weather/habit dependent. The system is centrally controlled where each building sets its desired temperature and communicates it to the central management unit.

The examined system is fully described with the following states. CHP related states are: P^{chp} - Active power output, Q^{chp} - Heat output, Q^{in} - Input heat and $\dot{m}^{\mathrm{chp}}$ - CHP plant supply mass flow rate. Building related states are: $\dot{m}_b$ - Mass flow rate of building b, T_b^{in} - Temperature inside building b. Heat network related states are: $\dot{m}_p$ - Mass flow rate along pipe p and T^{s} - District network supply temperature. Finally, the exchange related states are: $P^{\mathrm{grid}\pm}$ - Exchanged electric power (+ to grid, - from grid), $Q_m^{\mathrm{grid}\pm}$ - Exchanged heat power (+ to grid, - from grid) with market m, $\dot{m}_m^{\mathrm{grid}}$ - Mass flow rate of the heat exchanged with market m.

The examined system is affected by several parameters. These parameters can be grouped by the external environment. The first group are the weather/habit dependent parameters: T^{a} - Ambient temperature, I - Solar irradiation and P^{rl} - Residual electric load (Load minus PV production). The second group of parameters are the market related parameters: λ^{e} - electricity price, λ^{q} - heat price.

Finally, the examined system is controlled with the following control variables: $P^{\mathrm{chp,c}}$ - CHP power output control signal, $Q^{\mathrm{chp,c}}$ - CHP heat output control signal, $\dot{m}_b^{\mathrm{c}}$ - Building mass flow rate control signal. These signals are received by valve actuators which respond following their respective dynamics.

In the following, we append the parameters in vector

$$\Theta = (T^{\mathrm{a}}, I, P^{\mathrm{rl}}, \lambda^{\mathrm{e}}, \lambda^{\mathrm{q}}),$$

the system's states in vector

$$X = (P^{\mathrm{chp}}, Q^{\mathrm{chp}}, Q^{\mathrm{in}}, \dot{m}^{\mathrm{chp}}, \dot{m}_b, T_b^{\mathrm{in}}, T^{\mathrm{s}}, \dot{m}_p, P^{\mathrm{grid}\pm}, Q_m^{\mathrm{grid}\pm}, \dot{m}_m^{\mathrm{grid}}),$$

and the controls in vector

$$U = (P^{\mathrm{chp,c}}, Q^{\mathrm{chp,c}}, \dot{m}^{\mathrm{chp,c}}, \dot{m}_b^{\mathrm{c}}, \dot{m}_m^{\mathrm{grid,c}}).$$

For clarity, it is important to declare all sets used in the model. These are: Ω_n - Set of all nodes in a heating network, Ω_p - Set of all pipes in a heating network, Ω_b - Set of all buildings, Ω_m - Set of all heat markets.

A. Physical Model

The central component of the examined system is the cogeneration plant supplying both the heat and electric energy. Mathematical models of thermal power plants vary extensively depending on the design of the system in terms of re-heaters and pumps [16]. Since the focus in this paper is put on the

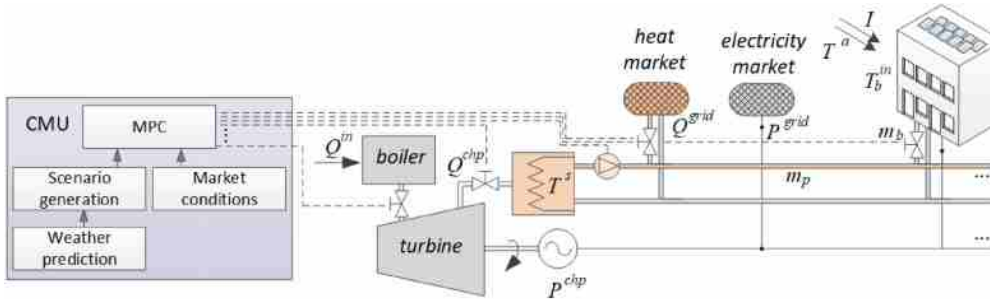

Fig. 1. CHP-based microgrid.

network and energy optimization, a simpler model with a single turbine will be adopted. Dynamics of such cogeneration plant are simpler and the following model describes the response of energy output to control signals:

$$\frac{\mathrm{d}P^{\mathrm{chp}}}{\mathrm{d}t} = \frac{1}{T_{\mathrm{chp,p}}}\left(P^{\mathrm{chp,c}} - P^{chp}\right) \quad (1a)$$

$$\frac{\mathrm{d}Q^{\mathrm{chp}}}{\mathrm{d}t} = \frac{1}{T_{\mathrm{chp,q}}}\left(Q^{\mathrm{chp,c}} - Q^{\mathrm{chp}}\right) \quad (1b)$$

where $T_{\mathrm{chp,p}}$ and $T_{\mathrm{chp,q}}$ are time constants of valves controlling the heat supply for electric and thermal energy conversions.

Depending on the extracted energy (for both heat and electric) the input heat will have to be corrected in order to achieve the desired extraction [17]. The input heat is determined with the extracted energy and the energy conversion efficiency of the plant:

$$Q^{\mathrm{in}} = \frac{P^{\mathrm{chp}} + Q^{\mathrm{chp}}}{\eta(P^{\mathrm{chp}}, Q^{\mathrm{chp}})} \quad (1c)$$

where Q^{in} is the input heat and η is the energy conversion efficiency.

It is indicated in (1c) that the energy conversion efficiency is a function of extracted energy in both forms. This function is typically described with a third order polynomial:

$$\begin{aligned}\eta = {}& \gamma_1 + \gamma_2 P^{chp} + \gamma_3 (P^{chp})^2 + \gamma_4 (P^{chp})^3 \\ & + (\gamma_5 + \gamma_6 (P^{chp}) + \gamma_7 (P^{chp})^2)(Q^{chp}) + \gamma_8 (Q^{chp})^2\end{aligned} \quad (1d)$$

Finally, in order to properly represent the energy conversion process it is necessary to include the operating range of the plant. Due to various characteristics of the energy conversion process, the operating range of a cogeneration plant is constrained to a specific region [18]. Fig. 2 depicts the energy conversion efficiency and a typical operating range of a cogeneration plant.

Mathematically, the operating range depicted in Fig. 2 can be described with a set of N linear inequalities:

$$A_i P^{\mathrm{chp}} + B_i Q^{\mathrm{chp}} + C_i \leq 0, \quad i = 1 \ldots N \quad (2)$$

The extracted heat enters the heat exchanger where it is being transferred to the circulating water which carries the heat through the supply network to the consumers. Consumers use this heat through radiators in order to maintain the desired temperature of the building. To do so, the heat needs to compensate for the loss of heat due to the exchange between the building and the environment. Upon supplying the buildings with heat, circulating water is returned to the heat exchanger in the plant where it is being reheated. In the following paragraphs, a mathematical description of the described process is given.

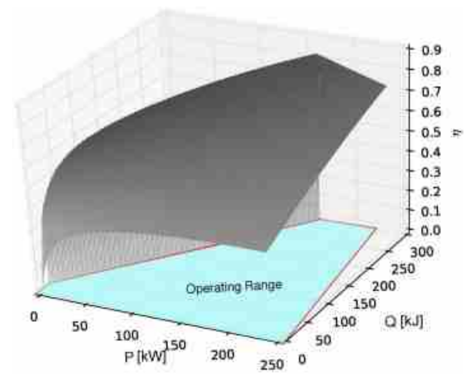

Fig. 2. Operating range and energy efficiency of the plant.

In order to develop a generic model of the heat supply system, it is necessary to introduce several generalizations. The heat supply system can be topologically seen as a directed graph $G = (N, B)$ with nodes and branches and respective matrices: Incidence matrix $\mathbf{A}$ connecting the nodes to the branches and loop incidence matrix $\mathbf{B}$ connecting the loops to the branches. Furthermore, two positional matrices and one positional vector are required to maintain the model's generic representation. The first positional matrix, denoted as $\mathbf{C}$, connects buildings to nodes. The second positional matrix, denoted as $\mathbf{D}$ connects heat markets to nodes. Finally, a vector $\mathbf{E}$ connects the CHP plant to a node.

The heat network is, in fact, a hydraulic network and it's states can be fully determined with two hydraulic laws [19]. Here, we will adopt a nodal formulation of these laws. The first law associated is the mass conservation principle expressed in:

$$\begin{aligned}&\sum_{p\in\Omega_p} A_{n,p}\dot{m}_p - \sum_{b\in\Omega_b} C_{n,b}\dot{m}_b \\ &\qquad + \sum_{m\in\Omega_m} D_{n,m}\dot{m}_m^{\mathrm{grid}} + E_n \dot{m}^{\mathrm{chp}} = 0, \quad \forall n,\end{aligned} \quad (3a)$$

The second law is the energy conservation principle expressed in:

$$\sum_{p\in\Omega_p} B_{l,p} K_p \dot{m}_p |\dot{m}_p| = 0, \quad \forall l \quad (3b)$$

where K_p is the pipeline p resistance coefficient.

The second set of equations are thermal equations determining the temperature dynamics in each building (details in [20]). Each node with connected building is characterized by the water entering the node with the temperature T^s and the mass flow rate $\dot{m}_b$ where it absorbs/releases heat and exits with the temperature T^r. The general mathematical description of the absorbed/released heat is:

$$Q_b = c_p \dot{m}_b (T^s - T^r). \tag{3c}$$

The absorbed/released heat determines the temperature dynamics in residential buildings. If we incorporate this expression into the general law of temperature dynamics in a closed system, the following thermal equation can be associated with each building:

$$\frac{\mathrm{d}T_b^{\mathrm{in}}}{\mathrm{d}t} = k_{1,b}(T^{\mathrm{a}} - T_b^{\mathrm{in}}) + k_{2,b}\dot{m}_b(T^{\mathrm{s}} - T^{\mathrm{r}}) + k_{3,b}A_b^{\mathrm{we}} I \tag{3d}$$

where $k_{1-3,b}$ are heat related coefficients and A_b^{we} is the building effective window area dependent on the building orientation.

In the case of the supply node, the temperature dynamics are similar. These dynamics are described with he following mathematical model:

$$\frac{\mathrm{d}T^{\mathrm{s}}}{\mathrm{d}t} = k_1^{\mathrm{chp}}(T^{\mathrm{a}} - T^{\mathrm{s}}) - k_2^{\mathrm{chp}}\dot{m}^{\mathrm{chp}}(T^{\mathrm{s}} - T^{\mathrm{r}}) + k_3^{\mathrm{chp}} Q^{\mathrm{chp}} \tag{3e}$$

The next set of equations is related to the market exchange. The exchanged heat is determined with the following equation:

$$Q_m^{\mathrm{grid}+} - Q_m^{\mathrm{grid}-} = c_p \dot{m}_m^{\mathrm{grid}}(T^{\mathrm{s}} - T^{\mathrm{r}}), \quad Q^{\mathrm{grid}\pm} \geq 0 \tag{3f}$$

where c_p is the specific heat of water.

The exchanged electric power is determined in:

$$P^{\mathrm{grid}+} - P^{\mathrm{grid}-} = P^{\mathrm{chp}} - P^{\mathrm{rl}}, \quad P^{\mathrm{grid}\pm} \geq 0 \tag{3g}$$

It is important to ensure the distinction between exported and imported heat/electric power in (3f) and (3g). This is required by the difference in prices for imported/exported power. This asymmetry is the consequence of the current market organization where the supply related auxiliary costs are transferred to the demand side [21]. This direction is preserved with the difference $Q^{\mathrm{grid}+} - Q^{\mathrm{grid}-}$, $P^{\mathrm{grid}+} - P^{\mathrm{grid}-}$ and the non-negative bounds, $Q_m^{\mathrm{grid}\pm} > 0$, $P^{\mathrm{grid}\pm} > 0$.

Finally, the valve actuators dynamics are defined in:

$$\frac{\mathrm{d}\dot{m}^{\mathrm{chp}}}{\mathrm{d}t} = \frac{1}{T_{\mathrm{valve}}^{\mathrm{chp}}}\left(\dot{m}^{\mathrm{chp,c}} - \dot{m}^{\mathrm{chp}}\right) \tag{3h}$$

$$\frac{\mathrm{d}\dot{m}_b}{\mathrm{d}t} = \frac{1}{T_{\mathrm{valve}}^{\mathrm{b}}}\left(\dot{m}_b^{\mathrm{c}} - \dot{m}_b\right) \tag{3i}$$

$$\frac{\mathrm{d}\dot{m}_m^{\mathrm{grid}}}{\mathrm{d}t} = \frac{1}{T_{\mathrm{valve}}^{\mathrm{grid}}}\left(\dot{m}_m^{\mathrm{grid,c}} - \dot{m}_m^{\mathrm{grid}}\right) \tag{3j}$$

where $\dot{m}$ and $\dot{m}^c$ denote the mass flow rate and the control signal for each valve (chp, building or grid), and T_{valve} is their respective time constant. This time constant is in the range of 0.1–5 seconds and, depending on the system sampling time, can be considered instantaneous.

III. Optimization Model

In order to develop an appropriate MPC framework, it is important to examine the decision process associated with the operational planning in a multi-energy microgrid. The most important requirement in the district heating operation is to maintain the desired temperature in residential buildings following the numerous external parameters affecting the building temperature. Furthermore, the electric demand of the buildings has to be satisfied as well. Supply of the heat and electricity demand is the primary objective of the multi-energy microgrid operation. Due to the flexibility available through the system's interconnection to the external markets, the second component of the decision process is economic in nature. Depending on the market circumstances, it might be cost-effective to buy heat/electric power from the external market or to produce and export. Furthermore, due to the price asymmetry, it might be cost-effective to minimize any trade and satisfy the demand within the microgrid.

A. Objective

The market organization adopted here assumes high temporal resolution trading. This means that the real-time operation follows trading immediately and the planned vs delivered energy deviations are negligible resulting in no imbalance penalty. This kind of trading is not a common practice at the moment. However, it is expected to become a common market practice in the future, following the development of smart grids [22].

The overall objective can be split in two distinct groups, the tracking and the economic objectives. The tracking objective is related to the temperature control inside the building where the desired temperature has to be maintained in accordance to the comfort preferences of the residents. For this purpose, the quadratic penalty is adopted in the objective. A more flexible temperature tracking could be adopted here [23]. However, tight temperature tracking allows for a clear analysis of the economic states dynamics and an exact comparison with the traditional approach. The economic objectives are related to the heat/electric market exchange and the production costs. All of these objectives can be defined as the minimization of the following function:

$$\begin{aligned} J(X(\cdot), U(\cdot), \Theta(\cdot)) :=& \\ &\alpha \sum_{b \in \Omega_b} \int_{\tau_0}^{\tau_{\mathrm{f}}} \underbrace{\left(T_b^{\mathrm{in}}(\tau) - T_b^{\mathrm{set}}(\tau)\right)^2}_{\text{desired building temperature}} \mathrm{d}\tau \\ &- \int_{\tau_0}^{\tau_{\mathrm{f}}} \underbrace{\left(\lambda^{\mathrm{e}+}(\tau) P^{\mathrm{grid}+}(\tau) - \lambda^{\mathrm{e}-}(\tau) P^{\mathrm{grid}-}(\tau)\right)}_{\text{electric power trading profit}} \mathrm{d}\tau \\ &- \int_{\tau_0}^{\tau_{\mathrm{f}}} \underbrace{\left(\lambda^{\mathrm{q}+}(\tau) Q^{\mathrm{grid}+}(\tau) - \lambda^{\mathrm{q}-}(\tau) Q^{\mathrm{grid}-}(\tau)\right)}_{\text{heat trading profit}} \mathrm{d}\tau \\ &+ \int_{\tau_0}^{\tau_{\mathrm{f}}} \underbrace{\lambda^{\mathrm{fuel}} Q^{\mathrm{in}}(\tau)}_{\text{fuel cost}} \mathrm{d}\tau. \end{aligned} \tag{4}$$

where $\lambda^{\mathrm{e}\pm}$ is the electricity sell/buy price, $\lambda^{\mathrm{q}\pm}$ is the heat sell/buy price, and λ^{fuel} is the fuel price. Weight α in (4) is necessary in order to set the importance of temperature tracking compared to economic part of the objective. Since we have put a high importance on temperature tracking, this weight will be set to 10^4.

B. Planning Horizon

In its strict formulation, the model predictive control is the finite-horizon approximation of the infinite-horizon control problem. Finding a suitable finite-horizon approximation is a difficult task, further complicated in the case of systems with long-term storages. On the other hand, the uncertainty of parameters on larger horizons allows for declaring higher importance on lower horizons. If an examined system has a specific periodicity in its nature, it is appropriate to organize the energy management accordingly. In the case of a district heating system, a characteristic daily periodicity can be recognized and the heat reservoirs are designed for this daily periodicity. Hence, the terminal constraint will be used to follow this periodicity:

$$T^{\mathrm{s}}(24h) = T^{\mathrm{s,full}} \tag{5}$$

where $T^{\mathrm{s,full}}$ is the system nominal supply temperature.

The planning horizon will span from t_0 to the end of the day. This means that the horizon will decrease as time passes until the end of the day when the new planning horizon starts.

C. Robust Formulation

The planning horizon at the beginning of the day is one day. This is a long horizon in terms of parameter forecast and the uncertainties in parameter prediction have to be taken into account in the MPC formulation. The robust formulation will "push" the control trajectories away from the boundary hull in order to enable the freedom to respond to the realization of different scenarios.

To achieve this, two extreme scenarios will be distinguished as the envelope of the complete set of scenarios. Such extreme trajectories in parameter realization have a very low probability and their purpose is to ensure the robustness. It is important to point out that the robust trajectories typically introduce economic loss. However, this loss is considered to be an acceptable trade-off for the resulting robustness. A more strict formulation could be adopted, where this economic trade-off could be formulated more precisely in terms of risk [24]. However, it is out of the scope of this paper to investigate this matter.

In order to achieve this robust formulation, each state, control, and parameter in the model will be formulated as scenario dependent, i.e. each state/control trajectory corresponds to each scenario trajectory of uncertain parameters. Each scenario is denoted with ξ and the set of all scenarios is $\Omega_\xi = \{exp, min, max\}$, where exp is the expected scenario while min and max are extreme scenarios. The expected scenario is related to the original deterministic problem formulated in (4). This scenario governs the expected economic interactions. On the other hand, extreme scenarios introduce robustness ensuring that the system can safely pass through extreme scenarios with fewer concerns for economics.

Now, Θ, X and U become Θ_ξ, X_ξ and U_ξ, and additional sets of constraints are added to the original problem. The complete optimization problem is now formulated as:

$$\min_{X_\xi(\cdot),U_\xi(\cdot)} \quad \pi_\xi \sum_{\xi\in\Omega_\xi} J_\xi(X_\xi(\cdot), U_\xi(\cdot), \Theta_\xi(\cdot)), \tag{6a}$$

$$\text{s.t.} \quad X_\xi(0) = \hat{X}(0), \tag{6b}$$

$$\dot{X}_\xi(\tau) = f(X_\xi(\tau), U_\xi(\tau), \Theta_\xi(\tau)), \tag{6c}$$

$$g(X_\xi(\tau), U_\xi(\tau), \Theta_\xi(\tau)) = 0, \tag{6d}$$

$$h(X_\xi(\tau), U_\xi(\tau), \Theta_\xi(\tau)) \leq 0, \tag{6e}$$

$$T_\xi^{\mathrm{s}}(24h) = T_\xi^{\mathrm{s,full}}, \tag{6f}$$

$$U_{exp}(\tau_0) = U_{min}(\tau_0) = U_{max}(\tau_0) \tag{6g}$$

In the complete formulation (6), π_ξ represents the weighting factor for each objective. This factor typically reflects the probability of each scenario. However, a more conservative approach could be implemented through higher weighting of the extreme scenarios. The last constraint in the reformulated problem ensures the unique control signal in the current control loop. This constraint connects all scenarios. Also, the coupling is performed through the tracking component of the objective. Namely, in each scenario, the objective is to maintain the desired temperature in buildings. Hence, the problem (6) is solved simultaneously for all scenarios.

D. Numerical Solution

The optimization problem defined in (6) is an example of the optimal control problem (OCP) governed by differential and algebraic equations (DAEs). Such problems are typically solved with a family of numerical methods referred to as direct methods [25]. These methods are based on the transformation of the original problem to a nonlinearly constrained optimization problem through discretization of the state and the control functions with respect to the temporal dimension. In this process, infinite-dimensional temporal space is approximated with a finite one. Three distinct methods in this family are single-shooting, multiple-shooting, and the collocation method. Single shooting approximates the entire trajectory using simulation and optimizes the parametrization of the control for the state trajectory. This method is suitable for simple control trajectories and is rarely used in complex systems. Multiple shooting breaks the trajectory into smaller segments and performs optimize/simulate sequences on each segment (single shooting on smaller segments). This increases the robustness making it suitable for complex systems. The collocation method approximates state trajectory as piece-wise polynomial and performs a single instance optimization with dynamics integrated into the NLP problem. The collocation method is also robust and suitable for complex systems. Compared to multiple shooting, collocation handles discontinuities of the control function better but results in an NLP problem with a higher number of variables [26]. Here, we will adopt the collocation method. The following paragraphs give a brief description of the collocation method.

Let us divide each control interval $[t_k, t_{k+1}]$ into an equidistant grid $t_{k,0} < t_{k,1} < \cdots < t_{k,ng}$ with $ng + 1$ points spaced

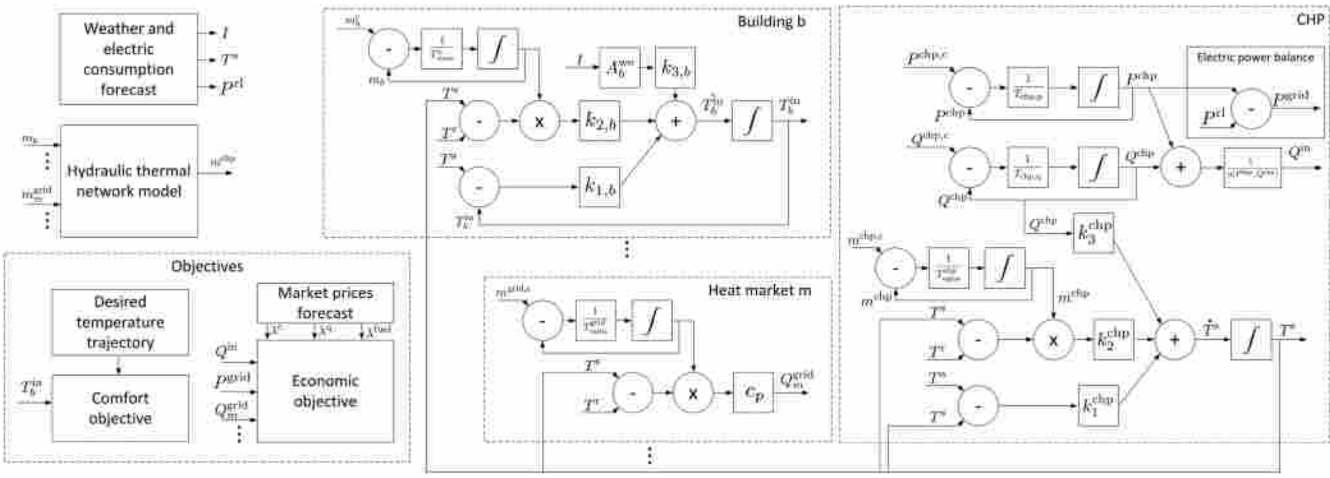

Fig. 3. Microgrid model block diagram representation.

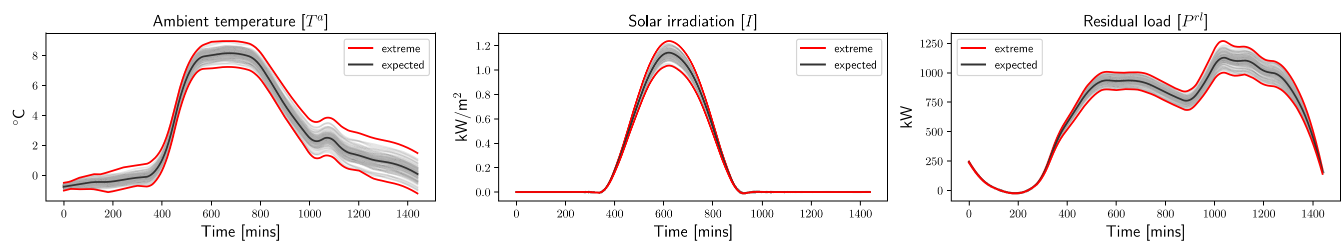

Fig. 4. Parameters scenarios.

by h. Each state is represented as a D-degree polynomial:

$$x_k(t) = \sum_{i=0}^{d} P_i\left(\frac{t - t_{k,j}}{h}\right) x_{k,j,i}, \quad t \in [t_{k,j}, t_{k,j+1}] \tag{7}$$

where, $x_{k,j,i}$ are polynomial coefficients and $P_i(\tau)$ is a Lagrangian polynomial basis of order d:

$$P_i(\tau) = \prod_{r=0, r\neq i}^{d} \frac{\tau - \tau_r}{\tau_i - \tau_r}, \quad \tau \in [0, 1] \tag{8}$$

Collocation points t_r are chosen through $Radau$ scheme. The state derivative is:

$$\frac{\mathrm{d}x_k(t)}{\mathrm{d}t} = \frac{1}{h} \sum_{i=0}^{d} P_i'(\tau) x_{k,j,i} \tag{9}$$

The dynamic constraints in implicit DAE formulation read as:

$$f_c\left(\frac{1}{h}\sum_{i=0}^{d} P_i'(\tau_i) x_{kji}, x_{kji}, u_k\right) = 0, \quad \begin{array}{c} k = 0, \ldots, N, \\ j = 0, \ldots, n_j, \\ i = 1, \ldots, d, \end{array} \tag{10}$$

In order to impose continuity it is necessary to connect all neighbouring intervals with:

$$\sum_{i=0}^{d} P_i(1) x_{kji} - x_{k,j+1,0} = 0, \quad \begin{array}{c} k = 0, \ldots, N, \\ j = 0, \ldots, n_j - 1 \end{array} \tag{11}$$

These approximations transform the original problem to nonlinear optimization problem. More details on the direct collocation method can be found in [27].

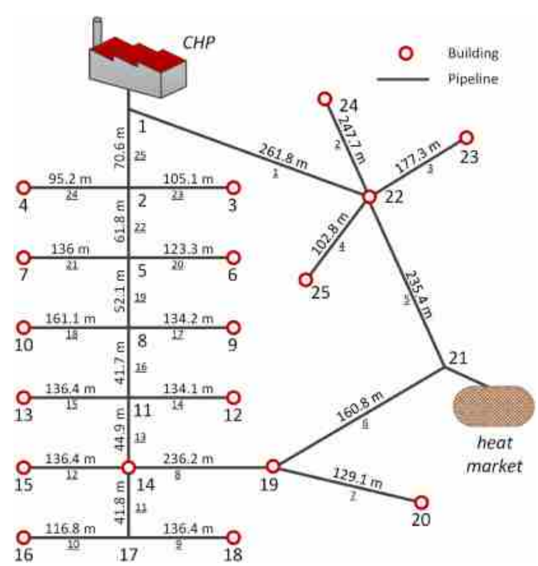

Fig. 5. Modified Barry Island heat network.

IV. Case Study

The MPC framework presented in this paper is validated on a case study of the modified Barry island heat network depicted in Fig. 5. The modifications introduced in this network are related to the addition of the heat exchange market.

The model parameters Θ are taken from [28] for temperature and solar irradiation while the residual load is obtained through

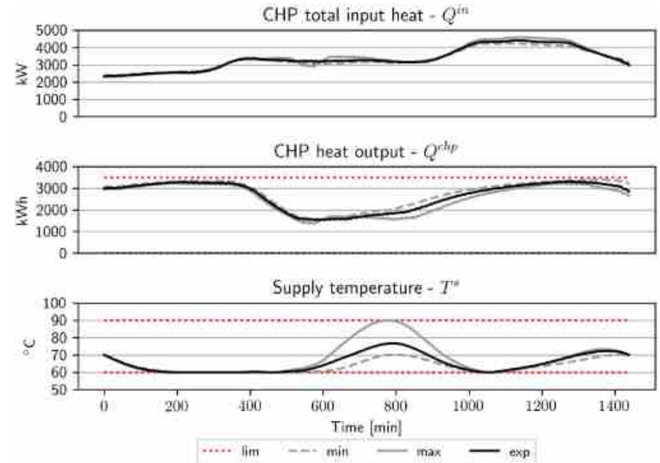

Fig. 6. Islanded regime - State trajectories for CHP input heat, CHP output heat, Supply temperature, and Grid exchange mass flow rate.

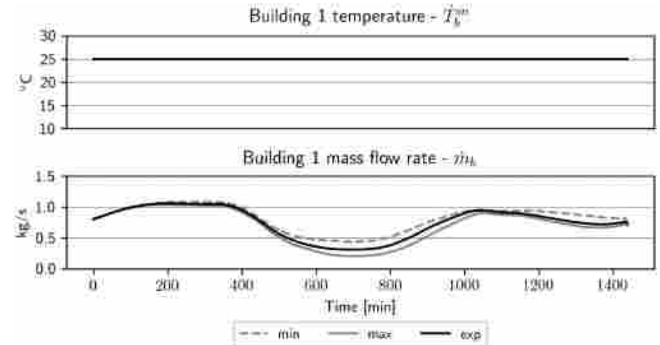

Fig. 7. Islanded regime - State/Control trajectories for Building 1 temperature and mass flow rate.

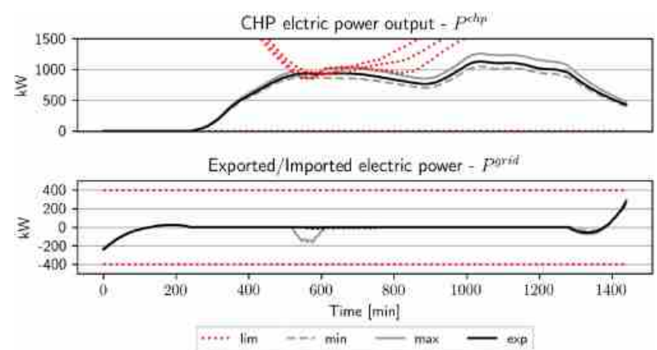

Fig. 8. Islanded regime - State/Control trajectories for CHP electric power output and Electric power exchange.

the scaling of typical load data. On top of these trajectories, a set of scenarios is simulated using autoregressive models to incorporate uncertainty in forecasting [29]. These scenarios are depicted in Fig. 4. As it is expressed in the robust formulation of the presented MPC framework, parameters affecting the building temperature and residual load are considered in *expected* (black line in Fig. 4) and *min/max* scenarios (red lines in Fig. 4). The *min/max* (red) scenarios are the outer hull of the complete set of scenarios. The desired building temperature is 25 °C. The electricity sell price is 60 € /MWh and the electricity buy price is 150 € /MWh. The heat sell/buy price is 10 € /MWh, and the fuel cost is 70 € /MWh.

The model is solved with IPOPT solver [30] in Python(PYOMO) environment [31] on a machine with Intel i7 2.7 GHz processor and 12 GB of RAM. The adopted sampling time of the model is 1 minute. The number of discretization steps is 100 with 3 collocation points on each segment. Typical solver time is in the range of 2 minutes for the first run. However, this time will be further reduced when the algorithm is implemented in a loop and the solutions can be transferred as initialization in each run. Since we are dealing with thermal systems with low temporal constants, this performance is satisfactory. The presented control scheme will be applied for two operation regimes: islanded mode and interconnected mode with respect to heat supply.

A. Islanded Regime

Fig. 6 depicts state trajectories for CHP input heat, CHP output heat, and supply temperature (grid exchange mass flow rate is zero in the islanded regime). The black line represents the expected scenario, gray lines represent extreme scenarios while the red line shows the operating range. The input heat is the result of heat and electric power output and the corresponding conversion efficiency. The second state is the CHP heat output. A characteristic dip can be noticed in the middle of the day. This dip is the result of the increase in the ambient temperature resulting in the heat demand decline. The opposite trend can be seen for the supply temperature. This means that the heat energy is stored in the CHP heat storage instead of an additional decrease in heat output which leads to a less efficient operating point.

Fig. 7 depicts trajectories for Building 1 temperature and mass flow rate. It can be seen that the desired temperature of 25 °C is maintained through variation of the building mass flow rate. Again, a characteristic dip can be noticed in the middle of the day following the increase in the ambient temperature. A single building is used for the clarity of the depiction, but the desired temperature is maintained in other buildings as well.

Fig. 8 depicts trajectories for CHP electric power output and Electric power exchange. The low selling price and the high buying price motivates the minimization of the exchange with the grid. However, due to limitations in CHP dynamics and the high inefficiency in low output operating points, a certain exchange is necessary. Another interesting phenomenon is the dynamic operating limits (red). Namely, the limit in electric power output depends on the current heat power output. Consequently, there is a conflict in operation objectives. Due to the decrease in heat power output following the increase in ambient temperature the limits in electric power decrease accordingly. On the other hand, during this period the electric consumption rises and the electric power follows it. This results in operation on the limits of the operating range. In the extreme consumption scenario, additional exchange with the grid can be noticed. Previously mentioned energy storing is the result of heat decrease avoidance that enables the higher limit in electric power output.

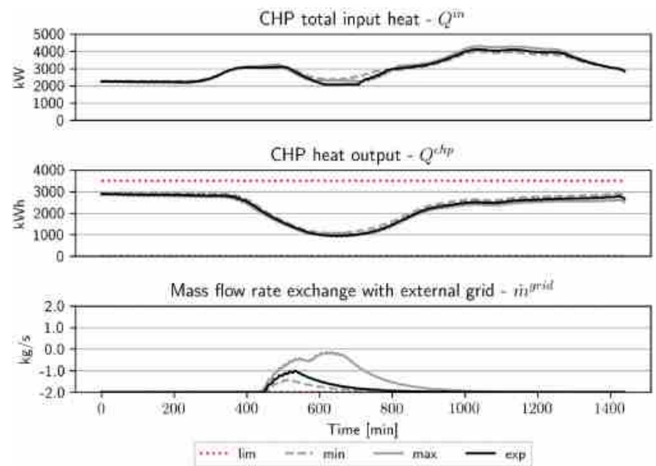

Fig. 9. Interconnected regime - State trajectories for CHP input heat, CHP output heat, Supply temperature, and Grid exchange mass flow rate.

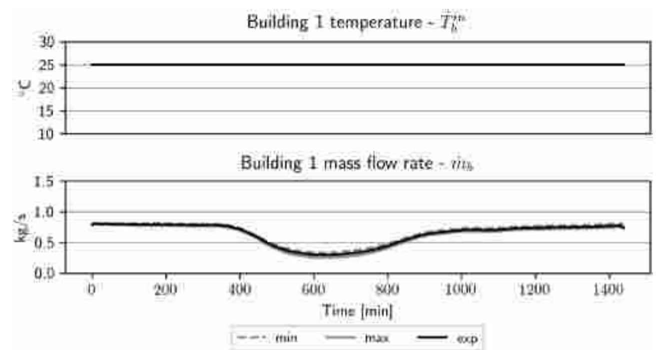

Fig. 10. Interconnected regime - State/Control trajectories for Building 1 temperature and mass flow rate.

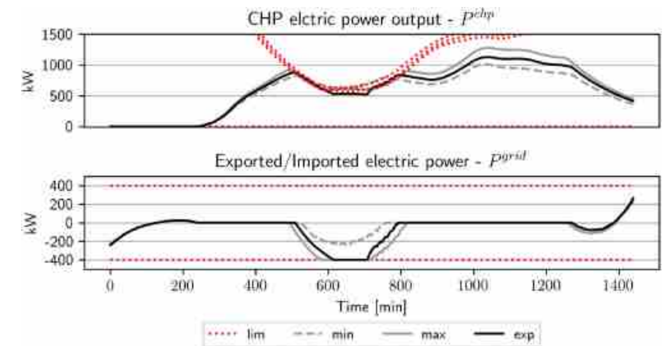

Fig. 11. Interconnected regime - State/Control trajectories for CHP electric power output and Electric power exchange.

TABLE I
ISLANDED REGIME

Cost	Q^{in}	Q^{grid}	P^{grid}	Total
Traditional	6579.5€	0€	-300€	6279.5€
ENMPC	5634.1€	0€	32.8€	5666.9€
Δ	-945.4€	0€	332.8€	-612.6€
			Δ[%]	-9.75%
INTERCONNECTED REGIME				
Traditional	5906.2€	205.5€	-126.4€	5985.3€
ENMPC	5012.9€	194.4€	232.5€	5439.8€
Δ	-893.3€	-11.1€	358.9€	-545.5€
			Δ[%]	-9.11%

B. Interconnected Regime

Let us assume an interconnected regime with limits of ± 2 kg/s. Another important assumption is the fixed supply temperature following the supply quality standard necessary in the exchange. The basic difference compared to the islanded regime is the availability of, in this case, cheaper source of heat. Hence, there is the motivation to maximize the heat import from the grid. Consequently, the mass flow rate of the import heat is maximal except for a brief period in the middle of the day as can be seen in the Fig. 9. This results in a decrease of the CHP heat output. The CHP heat output is minimized to a point where the conversion efficiency decreases and, also, the operating range of the electric side narrows.

Fig. 10 shows that, as it was the case with islanded regime, the temperature is kept on desired level. Although the heat demand is the same in both cases, due to the difference in supply temperature, the mass flow rate is slightly different in this case.

The electric market conditions are the same in both cases but the trajectories are different. Fig. 11 shows these trajectories. Again, there is a motivation for trading minimization due to the low selling and high buying price. The difference compared to the islanded operation is the increase in the electric power import in the middle of the day. This is the direct consequence of the change in the operating limits for the electric power following the decrease in heat output explained above. The economic loss introduced with this increase in electric power import is justified with the avoidance of fuel costs with cheaper heat import.

C. Performance Analysis

In order to point out the major benefits of the presented MPC framework, a comparison with the traditional approach is necessary. However, the examined framework is applicable in a rather novel environment. The multi-energy microgrids are a novel concept with few examples in traditional systems. Hence, we can only consider traditional district heating networks with decoupled energy systems. We will assume a typical management approach of satisfying heat demand with constant supply temperature while maximizing the electric power output.

The cost structure for traditional and ENMPC framework is shown in Table I. The profit form electric power exchange is higher in the traditional case. However, this profit cannot compensate for the increase in fuel costs for total input heat. The total costs are 612.6€ lower in the case of the ENMPC approach. This is a 9.75% decrease in costs on a daily level.Similar results can be seen in the case of the interconnected regime as well. The total costs are 545.5€ lower in the case of the ENMPC approach. This is a 9.11% decrease in costs on a daily level.

Although it is difficult to find an appropriate benchmark for novel concepts in energy supply, we have shown the benefits of economic model predictive control of multi-energy micro-grids. Significant savings can be achieved while maintaining the desired level of comfort.

V. Conclusion

In modern energy systems, it is necessary to consider the electric energy supply and heat energy supply jointly. This holds for smaller-scale energy systems and the multi-energy microgrid is considered in this paper. The central component of this microgrid is the CHP unit which connects the electric and heat supply systems.

We have shown that an energy management system based on the robust nonlinear economic model predictive control provides a comprehensive control framework with high model accuracy. Furthermore, introduced robustness prepares the system for extreme trajectories in parameter realization and hence ensures a safe operation. Economic character of the control objective models the economic consequences of the control trajectories. Such an approach seeks for the most economically feasible trajectories within the set of admissible trajectories. Further market liberalization initiatives will require economically motivated control/management approaches. Hence, the presented approach is in line with the expected energy system development. Important extension of the proposed model will be the distributed approach in system with several microgrids sharing common resources. Distributed control/management necessary introduces compromises and raises questions on fair access/usage of common infrastructure. This is one of the major issues in market liberalization initiatives.

The ongoing development in computational power allows for the implementation of detailed system models with complex numerical computations. On the other hand, it could be argued that the observed computational time might not be adequate if a larger system was considered. Hence, a practical validation is required in order to give a realistic value of the proposed approach. Possible future extensions of the proposed approach could integrate a detailed electrical model of the microgrid. The major challenge in this extension is the difference in temporal dynamics between electrical and thermal systems. Based upon observed computational time, such an extension could further challenge current computational capabilities.

References

[1] M. A. Rosen, M. N. Le, and I. Dincer, “Efficiency analysis of a cogeneration and district energy system,” *Appl. Thermal Eng.*, vol. 25, no. 1, pp. 147–159, Jan. 2005.

[2] L. Dong, H. Liu, and S. Riffat, “Development of small-scale and micro-scale biomass-fuelled CHP systems – A literature review,” *Appl. Thermal Eng.*, vol. 29, no. 11, pp. 2119–2126, Aug. 2009.

[3] M. Farrokhabadi *et al.*, “Microgrid stability definitions, analysis, and examples,” *IEEE Trans. Power Syst.*, vol. 35, no. 1, pp. 13–29, Jan. 2020.

[4] M. Ellis, H. Durand, and P. D. Christofides, “A tutorial review of economic model predictive control methods,” *J. Process Control*, vol. 24, no. 8, pp. 1156–1178, Aug. 2014.

[5] T. Wang, D. O’Neill, and H. Kamath, “Dynamic control and optimization of distributed energy resources in a microgrid,” *IEEE Trans. Smart Grid*, vol. 6, no. 6, pp. 2884–2894, Nov. 2015.

[6] T. Sun, J. Lu, Z. Li, D. L. Lubkeman, and N. Lu, “Modeling combined heat and power systems for microgrid applications,” *IEEE Trans. Smart Grid*, vol. 9, no. 5, pp. 4172–4180, 2018.

[7] D. E. Olivares, J. D. Lara, C. A. Caizares, and M. Kazerani, “Stochastic-predictive energy management system for isolated microgrids,” *IEEE Trans. Smart Grid*, vol. 6, no. 6, pp. 2681–2693, Nov. 2015.

[8] F. Valencia, J. Collado, D. Sez, and L. G. Marn, “Robust energy management system for a microgrid based on a fuzzy prediction interval model,” *IEEE Trans. Smart Grid*, vol. 7, no. 3, pp. 1486–1494, May 2016.

[9] M. Alipour, B. Mohammadi-Ivatloo, and K. Zare, “Stochastic scheduling of renewable and CHP-based microgrids,” *IEEE Trans. Ind. Informat.*, vol. 11, no. 5, pp. 1049–1058, Oct. 2015.

[10] H. Qi, H. Yue, J. Zhang, and S. Lo, “Optimal control of CHP plant integrated with load management on HVAC system in microgrid,” in *Proc. IEEE 15th Int. Conf. Control Automat.*, 2019, pp. 1073–1078.

[11] N. Nwulu, “Multi-objective optimization of a CHP-PV-battery islanded microgrid,” in *Proc. Int. Conf. Energy, Communication, Data Analytics Soft Comput.*, 2017, pp. 98–102.

[12] M. Houwing, R. R. Negenborn, P. W. Heijnen, B. De Schutter, and H. Hellendoorn, “Least-cost model predictive control of residential energy resources when applying CHP,” in *Proc. IEEE Lausanne Power Tech*, 2007, pp. 425–430.

[13] J. Vasilj, S. Gros, D. Jakus, and M. Zanon, “Day-ahead scheduling and real-time economic MPC of CHP unit in microgrid with smart buildings,” *IEEE Trans. Smart Grid*, vol. 10, no. 2, pp. 1992–2001, Mar. 2019.

[14] G. Darivianakis, A. Georghiou, R. S. Smith, and J. Lygeros, “The power of diversity: Data-driven robust predictive control for energy-efficient buildings and districts,” *IEEE Trans. Control Syst. Technol.*, vol. 27, no. 1, pp. 132–145, Jan. 2019.

[15] X. Liu, J. Wu, N. Jenkins, and A. Bagdanavicius, “Combined analysis of electricity and heat networks,” *Appl. Energy*, vol. 162, pp. 1238–1250, Jan. 2016.

[16] *Power System Stability and Control*, ser. EPRI power system engineering series. McGraw-Hill, 1994.

[17] A. Wood, B. Wollenberg, and G. Sheblé, *Power Generation, Operation, and Control*. New York, NY, USA: Wiley, 2013.

[18] A. Rong and R. Lahdelma, “Efficient algorithms for combined heat and power production planning under the deregulated electricity market,” *Eur. J. Oper. Res.*, vol. 176, no. 2, pp. 1219–1245, Feb. 2007.

[19] E. Cabrera, J. Garcia-Serra, and P. Iglesias, *Modelling Water Distribution Networks: From Steady Flow to Water Hammer. In: Improving Efficiency and Reliability in Water Distribution Systems*. Berlin, Germany: Springer, 1995.

[20] P. Bacher and H. Madsen, “Identifying suitable models for the heat dynamics of buildings,” *Energy Buildings*, vol. 43, no. 7, pp. 1511–1522, Jul. 2011.

[21] K. Bhattacharya, M. Bollen, and J. Daalder, *Operation of Restructured Power Systems*, ser. Power Electronics and Power Systems. Springer U.S., 2001.

[22] Y. Ding, S. Pineda, P. Nyeng, J. stergaard, E. M. Larsen, and Q. Wu, “Real-time market concept architecture for Ecogrid EU–A prototype for european smart grids,” *IEEE Trans. Smart Grid*, vol. 4, no. 4, pp. 2006–2016, 2013.

[23] E. T. Maddalena, Y. Lian, and C. N. Jones, “Data-driven methods for building control a review and promising future directions,” *Control Eng. Pract.*, vol. 95, 2020. Art. no. 104211, [Online]. Available: http://www.sciencedirect.com/science/article/pii/S0967066119301832

[24] Z. Xu, Z. Hu, Y. Song, and J. Wang, “Risk-averse optimal bidding strategy for demand-side resource aggregators in day-ahead electricity markets under uncertainty,” *IEEE Trans. Smart Grid*, vol. 8, no. 1, pp. 96–105, Jan. 2017.

[25] M. Zanon, A. Boccia, V. Palma, S. Parenti, and I. Xausa, *Direct Optimal Control and Model Predictive Control*, Cham: Springer International Publishing, vol. 2180, Sep. 2017, pp. 263–382.

[26] J. T. Betts, *Practical Methods for Optimal Control and Estimation Using Nonlinear Programming*, 2nd ed. Society for Industrial and Applied Mathematics, 2010. [Online]. Available: https://epubs.siam.org/doi/abs/10.1137/1.9780898718577

[27] L. T. Biegler, *Nonlinear Programming: Concepts, Algorithms, and Applications to Chemical Processes*. USA: Soc. Industrial Appl. Math., 2010.

[28] *Deutcher Wetterdienst - Climate Data Center*. [Online]. Avaiable: www.dwd.de

[29] J. Vasilj, P. Sarajcev, and D. Jakus, “Estimating future balancing power requirements in windpv power system,” *Renewable Energy*, vol. 99, pp. 369–378, 2016.

[30] A. Wächter and L. T. Biegler, “On the implementation of a primal-dual interior point filter line search algorithm for large-scale nonlinear programming,” *Math. Program.*, vol. 106, no. 1, pp. 25–57, Mar. 2006.

[31] W. E. Hart, J.-P. Watson, and D. L. Woodruff, “Pyomo: Modeling and solving mathematical programs in python,” *Math. Program. Comput.*, vol. 3, no. 3, pp. 219–260, Aug. 2011.